United States
Department of
Agriculture

Forest Service
Forest Pest
Management

Davis, CA

FSCBG TECHNICAL MANUAL

FPM 92-4
March 1992

FPM 92-4
C. D. I. Report No. 91-01
March 1992

FSCBG TECHNICAL MANUAL

Prepared by:

Milton E. Teske

Continuum Dynamics, Inc.
P. O. Box 3073
Princeton, NJ 08543

Contract No. 53-0343-9-00076

Prepared for:

USDA Forest Service
Forest Pest Management
2121C Second Street, Suite 102
Davis, CA 95616
(916) 758-4600

John W. Barry
Project Officer

Summary

The version of FSCBG (Forest Service Cramer Barry Grim) described in this technical manual combines and implements mathematical models for aircraft wake effects, gaussian line source dispersion, droplet evaporation, canopy penetration, and ground and canopy deposition. FSCBG is designed to account for the atmospheric dispersion, transport, and deposition of all aerial spray material from the time of release until the spray material is either deposited or, in the case of spray drift, until the spray concentration and deposition levels become insignificant. Specific calculations made by FSCBG include spray concentrations and dosages above and within forest canopies as well as the spray deposition within and below forest canopies, resulting from aerial spray releases made along single or multiple flight paths. This document serves as the technical resource manual for FSCBG.

Table of Contents

1. Introduction

The FSCBG (Forest Service Cramer Barry Grim) computer model for predicting aircraft spray dispersion and deposition above and within forest canopies results from the merging of models for simulating the effect of the aircraft wake on the behavior of released spray material, the penetration of spray material into a forest canopy, and determining optimum swath widths, application rates, and aircraft altitudes to achieve specific objectives. FSCBG combines and implements mathematical models for aircraft wake effects, gaussian line source dispersion, droplet evaporation, canopy penetration, and ground and canopy deposition. The USDA Forest Service selectively uses aerial spray applications to control forest pests while the U. S. Army is interested in assessing the effectiveness of chemical and biological defensive strategies. Both agencies are interested in achieving a more complete understanding of the behavior of spray material from the time spray is released from the aircraft until it has been deposited or, in the case of spray drift, diffused to concentration/dosage levels that are environmentally insignificant. Because mathematical spray dispersion models are useful in determining interactions of the many factors affecting spray operations, the USDA Forest Service and U. S. Army have supported the application and development of these models over the last twenty years.

Each principal model section of FSCBG is reviewed in subsequent chapters: meteorology (chapter 2); evaporation (chapter 3); canopy penetration (chapter 4); near wake particle trajectories (chapter 5); and dispersion (chapter 6). This manual is an extension of portions of Dumbauld, Bjorklund and Saterlie 1980 and Bjorklund, Bowman and Dodd 1988.

2. Meteorology

All meteorological data are entered in tables in FSCBG, and then curve fits or averages are taken to arrive at typical data levels in open terrain or within a canopy. Wind speed fits a functional three-layer dependence, while all other variables (temperature, relative humidity and wind direction) fit a height-weighted mean value over the depth of interest.

The functional form of the wind speed variation with height depends on the regime involved. In open terrain where there is no canopy, or at heights greater than twice the height of the canopy, the familiar power law is used. The power-law profile gives the wind speed at any height between the surface and the height of the surface mixing layer H_m as

$$u = u_r \left(\frac{z}{z_r} \right)^p \tag{2-1}$$

where z_r is the reference height where the reference wind speed u_r is measured, p is the power law exponent, z is the height of interest, and u is the resultant wind speed. In FSCBG z_r is set equal to 10 meters.

Cionco (1965) developed a wind profile law for describing the variation of wind speed within vegetative canopies

$$u = u_c \exp\left[\alpha_c \left(\frac{z}{H_c} - 1 \right) \right] \tag{2-2}$$

for any height z up to H_c, the height of the top of the canopy. The parameter α_c is called the canopy index, and u_c is the wind speed at the top of the canopy.

A transition region exists (Bergen 1971) between the top of the canopy and twice the height of the canopy where the variation of wind speed with height may be given by the well-known logarithmic profile

$$u = \frac{u^*}{k} \ln\left(\frac{z - d + z_o}{z_o} \right) \tag{2-3}$$

where u^* is the friction velocity, d is the displacement height, and z_o is the roughness length. In FSCBG d and z_o are set equal to $0.7\,H_c$ and $0.14\,H_c$ respectively (from Dumbauld and Bowers 1983).

After manipulation, these three equations may be expressed in the form

$$f(u) = a + b\, g(z) \tag{2-4}$$

where $f(u)$ is a suitable function of wind speed and $g(z)$ is a suitable function of height. In this way the coefficients a and b in Equation (2-4) may be linear least squares fit to user-entered data. In FSCBG the user-entered wind speed data in open terrain are fitted to Equation (2-1) with the manipulation

$$\ln u = \ln u_r + p \ln\left(\frac{z}{z_r}\right) \tag{2-5}$$

with linear least squares determining u_r and p. The wind speed data within a canopy are fitted to Equation (2-2) with the manipulation

$$\ln u = \ln u_c - \alpha_c + \alpha_c\left(\frac{z}{H_c}\right) \tag{2-6}$$

with linear least squares determining u_c and α_c. Continuity of wind speed at the top of the canopy and at the top of the transition region results in unique coefficients for Equation (2-3) with the manipulation

$$u = \frac{u^*}{k} \ln\left(\frac{H_c}{z_o}\right) + \frac{u^*}{k} \ln\left(\frac{z - d + z_o}{H_c}\right) \tag{2-7}$$

and consistency at $z = H_c$ and $z = 2\, H_c$. In this way an analytic description of the wind speed variation with height is developed from user-entered data.

If the user enters wind speed data at only a single height, or defines the layer average wind speed, Equations (2-1) and (2-2) must be integrated in the vertical direction to compute the average wind speed and deduce u_r and p in Equation (2-1), and u_c and α_c in Equation (2-2). With these values in hand, continuity of the wind speed at $z = H_c$ and $z = 2\, H_c$ may be invoked to determine u^* / k in Equation (2-3).

Integration of Equation (2-1) for the average wind speed $\bar{u}$ in open terrain yields

$$u_r = \frac{\bar{u}\,(H_m - z_b)\, z_r^{\,p}\,(p + 1)}{H_m^{\,p+1} - z_b^{\,p+1}} \tag{2-8}$$

where z_b is assumed equal to 2 meters. The value of u_r (or $\bar{u}$) then depends on the value of the power law exponent p.

Integration of Equation (2-2) for the average wind speed $\bar{u}$ within a canopy yields

$$u_C = \frac{\alpha_C \bar{u}}{(1 - \exp(-\alpha_C))} \tag{2-9}$$

where α_C is determined (Dumbauld and Bowers 1983) by requiring wind speed and its derivative to be continuous at the top of the canopy into the transition region (at $z = H_C$). This requirement yields

$$\alpha_C = \frac{H_C}{(H_C - d + z_O)\ln\left(\frac{H_C - d + z_O}{z_O}\right)} = 1.985 \tag{2-10}$$

for the values of d and z_O assumed in FSCBG. Equation (2-9) then shows that the wind speed u_C at the top of the canopy equals 2.3 times the mean wind speed within the canopy.

The power law exponent p is determined from tables in Dumbauld and Bowers 1983 fit by a hyperbolic multiquadric approach (Hardy 1971) to determine smooth first and second derivatives with respect to wind speed and net radiation index. Evaluation through the table is performed by Gregory square (Barnhill 1977 and Gregory 1974). Bjorklund, Bowman and Dumbauld 1984 extend this technique to include evaluation of typical wind elevation angle, wind azimuth angle and surface mixing layer height to recover these needed meteorological values smoothly.

3. Evaporation

In FSCBG the time rate of change of drop diameter due to evaporation is based on the expression (Fuchs 1959; Beard and Pruppacher 1971; Goering, Bode and Gebhardt 1972; and Williamson and Threadgill 1974)

$$\frac{dD}{dt} = -\frac{4 M_\ell D_v \rho_A \left(e_s - e_\infty \right)}{M_m D \rho_\ell \left(P_A - e_s \right)} f_v \qquad (3\text{-}1)$$

where

M_ℓ = molecular weight of evaporating vapor from the drop (gm/mole)

M_m = mean molecular weight of the resulting vapor-air mixture, approximated by air (M_A gm/mole)

D_v = molecular diffusivity of the evaporating vapor in air at the drop temperature (cm^2/sec)

D = drop diameter (cm)

ρ_A = air density (gm/cm^3)

ρ_ℓ = density of the drop (gm/cm^3)

e_s = partial pressure of the evaporating vapor at the drop surface (mb)

e_∞ = partial pressure of the evaporating vapor far from the drop (mb)

P_A = air pressure (mb)

f_v = ventilation factor (no units)

Air density is calculated from the relationship

$$\rho_A = \frac{P_A M_A}{R^* T_v} \qquad (3\text{-}2)$$

where R^* is the universal gas constant and T_v is given in terms of the mixing ratio r_∞ (Beard and Pruppacher 1971)

$$T_V = \frac{T_A\left(1 + \frac{r_\infty}{0.62197}\right)}{1 + r_\infty} \tag{3-3}$$

where

T_A = air temperature (deg K)

$$r_\infty = \frac{0.62197\, e_\infty}{P_A - e_\infty} \tag{3-4}$$

The diffusivity D_V of vapor into air at the temperature of the surface of the drop T_r depends on the liquid being considered. For water drops FSCBG uses the expression (Hall and Pruppacher 1976)

$$D_V = 0.211\left[\frac{T_r}{T_o}\right]^{1.94}\left[\frac{P_o}{P_A}\right] \tag{3-5}$$

where $T_o = 273.15$ deg K, $P_o = 1013.25$ mb and T_r is determined from the relation

$$T_r = T_A - \frac{L\, D_V\, M_\ell\left(e_S - e_\infty\right)}{k\, R^*\, T_f} \tag{3-6}$$

where (Beard and Pruppacher 1971 and Pruppacher and Rasmussen 1979)

L = latent heat of vaporization (cal/gm)

$$= 597.3\left[\frac{T_o}{T_r}\right]^{\alpha} \tag{3-7}$$

$$\alpha = 0.107 + 0.000367\, T_r \tag{3-8}$$

k = thermal conductivity (cal/cm-sec-deg K)

$$= k_d\left[1 - \left(1.17 - \frac{1.02\, k_V}{k_d}\right)\left(\frac{e_\infty}{P_A}\right)\right] \tag{3-9}$$

$$k_d = 0.00001 [5.69 + 0.017 (T_r - T_o)] \quad (3\text{-}10)$$

$$k_v = 0.00001 [3.78 + 0.020 (T_r - T_o)] \quad (3\text{-}11)$$

$$T_f = \frac{T_r + T_A}{2} \quad (3\text{-}12)$$

The partial pressure e_s is defined by the expression (Rasmussen 1978)

$$e_s = \beta \left[\frac{575.0466 + 31.82291\, T_i + 1.296028\, T_i^2}{93.51611 - T_i} \right] \quad (3\text{-}13)$$

where

$$T_i = T_r - T_o \quad (3\text{-}14)$$

$$\beta = 1$$

The vapor pressure e_∞ is also obtained from Equation (3-13) when T_r is replaced by T_A in Equation (3-14) and β is replaced by the relative humidity expressed in fractional form. Equations (3-5) through (3-13) are solved by iteration in FSCBG to determine the drop temperature, vapor pressure at the drop surface and diffusivity. Then Equation (3-1) is solved for the diameter change.

The ventilation factor f_v for water is given (Pruppacher and Rasmussen 1979) by

$$f_v = 0.78 + 0.308\, Sc^{1/3}\, Re^{1/2} \quad (3\text{-}15)$$

for

$$1.4 < Sc^{1/3}\, Re^{1/2} \leq 51.4$$

and

$$f_v = 1.0 + 0.108 \left(Sc^{1/3}\, Re^{1/2} \right)^2 \quad (3\text{-}16)$$

for

$$0 \le Sc^{1/3} Re^{1/2} \le 1.4$$

where

Re = Reynolds number

$$= \frac{V D \rho_A}{\mu_A} \tag{3-17}$$

Sc = Schmidt number

$$= \frac{\mu_A}{D_V \rho_A} \tag{3-18}$$

V = terminal settling velocity (cm/sec; McDonald 1960)

μ_A = absolute viscosity of air (gm/cm-sec; Beard and Pruppacher 1971)

$$= \frac{0.076342}{T_A + 296.16} \left(\frac{T_A}{296.16} \right)^{3/2} \tag{3-19}$$

FSCBG can also theoretically determine the time rate change of drop diameter for non-water drops. However, for this option to work, additional input information is required. In this case the drop temperature and vapor pressure at the surface of the drop are calculated from the expression (Beard and Pruppacher 1971)

$$\exp(B - C/T_r) - e_\infty = \left(\frac{k}{C_f D_V L M_\ell} \right) (T_A - T_r)[P_A - \exp(B - C/T_r)] \tag{3-20}$$

where

C_f = molal concentration of the liquid (moles/cm^3)

and

B, C = constants obtained from tables expressing variations of vapor pressure with temperature (for example, Weast 1981 with some manipulation into compatible units)

Values of k, D_v and L for non-water drops must be specified by the user. When the parameters required by Equation (3-20) have been specified, FSCBG uses a Newton-Raphson iteration technique to determine the drop temperature, vapor pressure and the time rate change of diameter, using the following expression (Fuchs 1959) for the ventilation factor

$$f_v = \frac{1}{2} Sh \tag{3-21}$$

where

$$\begin{aligned} Sh &= \text{Sherwood number} \\ &= 2 (1 + \alpha Sc^{1/3} Re^{1/2}) \end{aligned} \tag{3-22}$$

with $\alpha = 0.3$ (Williamson and Threadgill 1974).

Results obtained using the evaporation model for open terrain calculations are fitted to a quadratic by least-squares over the time period required for the drop to evaporate to a diameter of 5 micrometers or reach a settling velocity of 0.02 cm/sec, whichever is greater. Within canopy calculations are fitted to a quadratic over the time period required for the drop to travel from the top of the canopy to the ground.

4. Canopy

The probability that a drop will penetrate a canopy depends on the total number and size of vegetative elements encountered (Rafferty and Bowers 1989). If the orientation of the vegetative elements is assumed to be random, then the probability of penetration for a given path length will be the same for all directions. In FSCBG P_p, the probability of penetration, is defined as the probability that a drop traversing a horizontal trajectory will penetrate a typical single tree envelope. The value of P_p is assigned for each tree type based on foliage density and envelope dimensions.

In the analytic canopy penetration algorithm the height of the canopy is divided into twelve layers and an average tree diameter is computed for each layer. Each tree is represented in the k^{th} layer by a cylinder of diameter W_k and height Δz_k. The average length of a drop trajectory through this cylindrical envelope is

$$L_k = \frac{\frac{\pi}{4} W_k \Delta z_k \left(u_k^2 + V^2 \right)^{1/2}}{\frac{\pi}{4} W_k V + u_k \Delta z_k} \qquad (4\text{-}1)$$

where

u_k = wind speed (horizontal)

V = terminal settling velocity (vertical)

In the limit of wind speed u_k approaching zero, L_k equals Δz_k. Similarly, in the limit of settling velocity V approaching zero, L_k equals $\pi W_k / 4$, the mean horizontal path length through a circle of diameter W_k. A correction factor α may be defined as $L_k / (\pi W_k / 4)$, designating the number of mean horizontal path lengths traversed by an inclined drop trajectory while penetrating a cylindrical tree. Thus, the probability that a particle will penetrate one tree is given by

$$P_k = 1 - E\left(1 - P_p^{\alpha} \right) \qquad (4\text{-}2)$$

where

E = collection efficiency

The analytic canopy penetration algorithm assumes that the probability of a drop encountering a randomly placed tree envelope is equal to the fraction of the horizontal area effectively occupied by trees. If the drops fall vertically, this probability is simply the fraction of the horizontal area occupied by trees; this fraction must be increased to account for horizontal drop transport. The increase in the effective horizontal area of a single tree is given by the product of W_k and the downwind distance a drop travels while falling through Δz_k. The resulting probability of encountering a tree envelope is

$$f_k = \left(\frac{\pi}{4} W_k^2 + \frac{u_k \; W_k \, \Delta z_k}{V} \right) \rho_t \qquad (4\text{-}3)$$

where ρ_t is the tree density (number of stems per unit area). In Equation (4-3) it is possible for f_k to exceed unity. The overall probability of a drop penetrating a layer is then given by

$$P_{Tk} = [\, 1 - F_k (1 - P_k)] \, P_k^{I_k} \qquad (4\text{-}4)$$

where P_k is from Equation (4-2), and I_k and F_k are the integer and fractional parts of f_k, respectively. For example, if f_k equals 2.4, I_k equals 2 and F_k equals 4. In this case, six-tenths of the drops penetrate two trees and the remaining four-tenths penetrate three trees.

The collection efficiency E is determined by impaction and interception with cylindrical representations of the tree elements. Two parameters are evaluated

$$St = \text{Stokes number} = \frac{\rho_\ell D^2 U}{9 \mu_A D_t} \qquad (4\text{-}5)$$

$$\phi = \frac{9 \rho_A^2 D_t U}{\mu_A \rho_\ell} \qquad (4\text{-}6)$$

where

ρ_ℓ = density of the drop (gm/cm^3)

D = drop diameter (cm)

U = particle speed (cm/sec)

μ_A = absolute viscosity of air (gm/cm-sec)

D_t = characteristic size of a tree element (cm)

ρ_A = air density (gm/cm^3)

St and ϕ are then used with the cylindrical impaction curves of Golovin and Putnam 1962 to determine the impaction efficiency E_i (Figure 4-1). This efficiency is augmented by an interception effect (Pulley and Walters 1990), which for a cylinder gives

$$E = E_i + C\frac{D}{D_t} \tag{4-7}$$

with

$$C = 1 + 0.33\ St^{-0.96} \tag{4-8}$$

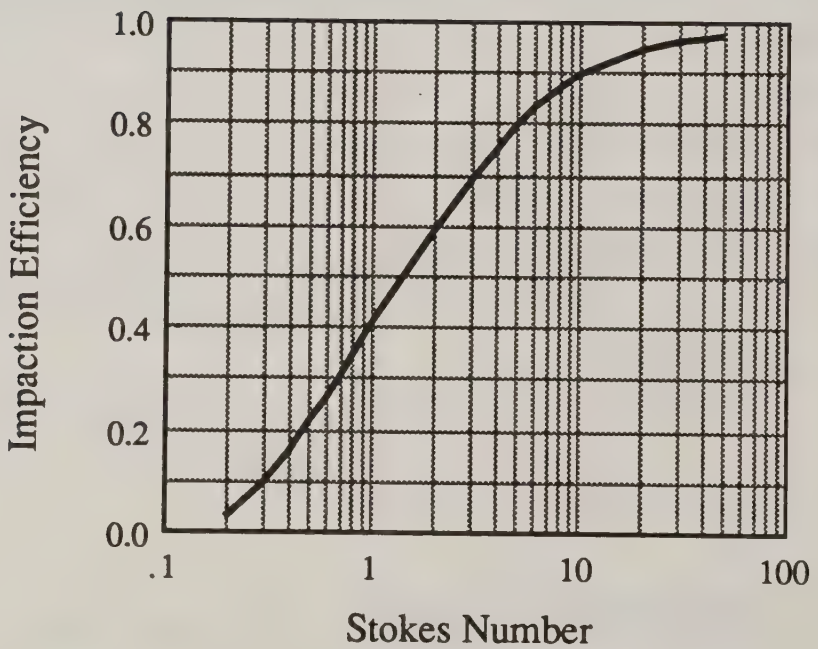

Figure 4-1. Cylindrical impaction efficiency curve for $\phi = 0$ (Golovin and Putnam 1962).

5. Near Wake

A Lagrangian approach is used to develop the equations of motion of discrete particles released from aircraft, with the resulting set of ordinary differential equations solved exactly from step to step. The formulation of the near-wake equations, particularly the ensemble averaged approach used to develop turbulent properties of the particle-atmospheric interaction, is detailed in Bilanin and Teske 1984. The near-wake implementation is consistent with AGDISP (Teske 1990).

Released material is assumed to be spherically shaped. Particle flight path as a function of time after release is computed as the locations (X,Y,Z) for all particles included in the simulation; velocity is denoted by (U,V,W) . The interaction of the material with the turbulence in the environment creates turbulent correlation functions for the position and velocity, $< yv >$ and $< zw >$; for the velocity variance, $< vv >$ and $< ww >$; and for the position variance, $< yy >$ and $< zz >$. The square root of these last two variables gives the horizontal and vertical standard deviations of the material motion about the mean described by Y and Z .

EQUATIONS OF MOTION

In the near wake, released material is assumed to be influenced by two forces: weight and aerodynamic drag. The governing equations are derived in Bilanin and Teske 1984 and repeated here for completeness

Mean Equations:

$$\frac{d^2X_i}{dt^2} = (U_i - V_i) \left[\frac{1}{\tau_p} \right] + g_i \qquad (5\text{-}1)$$

$$\frac{dX_i}{dt} = V_i \qquad (5\text{-}2)$$

Turbulent Correlations:

$$\frac{d}{dt} < x_i x_i > = 2 < x_i v_i > \qquad (5\text{-}3)$$

$$\frac{d}{dt} < x_i v_i > = \left(< x_i u_i > - < x_i v_i > \right) \left[\frac{1}{\tau_p} \right] + < v_i v_i > \qquad (5\text{-}4)$$

$$\frac{d}{dt} < v_i v_i > = 2 \left(< u_i v_i > - < v_i v_i > \right) \left[\frac{1}{\tau_p} \right] \qquad (5\text{-}5)$$

In Equations (5-1) to (5-5), X_i, V_i and U_i are the ensemble averaged ith components of material position, material velocity and local fluid velocity, respectively, while x_i, v_i and u_i are the fluctuating ith components of material position, material velocity and local fluid velocity, respectively; t is time and g_i is the gravity vector.

Inherent in the equations is a relaxation time τ_p which is essentially the e-folding time for the released particle to come up to speed with the local fluid velocity (for V_i to approach and equal U_i). The relaxation time is defined as

$$\tau_p = \frac{4}{3} \frac{D \rho_\ell}{C_D V_{rel} \rho_A} \tag{5-6}$$

where D is the diameter of the drop, ρ_ℓ is its density, ρ_A is the density of air, V_{rel} is the relative velocity between the material velocity and the local background velocity, and C_D is the particle drag coefficient. The semi-empirical formula for C_D (Langmuir and Blodgett 1946) is

$$C_D = \frac{24}{Re}\left(1 + 0.197\, Re^{0.63} + 0.00026\, Re^{1.38} \right) \tag{5-7}$$

where Re is the Reynolds number defined as

$$Re = \frac{V_{rel} D \rho_A}{\mu_A} \tag{5-8}$$

with

V_{rel} = relative velocity = $|U_i - V_i|$

μ_A = absolute viscosity of air

Equations (5-1) to (5-5) cannot be solved without specifying relationships for the quantities $< x_i u_i >$ and $< u_i v_i >$, the correlations of the particle position and particle velocity fluctuations, respectively, with the local fluid velocity fluctuation. These expressions are developed by integrating their ensemble averaged frequency spectra using a spectral density function for transverse velocity fluctuations in isotropic turbulence (von Karman and Howarth 1938). The results (detailed in Bilanin and Teske 1984) give

$$< x_i u_i > = \frac{q^2}{3}\left[-\tau_p K + \frac{\tau_\tau}{2} \right] \qquad (5\text{-}9)$$

$$< u_i v_i > = \frac{q^2}{3} K \qquad (5\text{-}10)$$

with

q^2 = mean square turbulence level

= $< uu > + < vv > + < ww >$

$$K = \frac{1}{2} \frac{\left[3 - \left(\frac{\tau_p}{\tau_\tau}\right)^2 \right]\left[1 - \frac{\tau_p}{\tau_\tau} \right] + \left(\frac{\tau_p}{\tau_\tau}\right)^2 - 1}{\left[1 - \left(\frac{\tau_p}{\tau_\tau}\right)^2 \right]^2} \qquad (5\text{-}11)$$

and τ_τ is the travel time of the particle through a turbulent eddy of scale Λ, adjusted for the passive tracer limit

$$\tau_\tau = \frac{\Lambda}{V_{rel} + \frac{3}{8} q} \qquad (5\text{-}12)$$

With the position and velocity information available for all released material at any time during the simulation, Equations (5-1) to (5-5) may be integrated exactly for the solution at the next time step (Teske 1988). The mean Equations (5-1) and (5-2) may be combined to give

$$\frac{d^2 X_i}{dt^2} + \frac{1}{\tau_p} \frac{dX_i}{dt} = \frac{U_i}{\tau_p} + g_i \qquad (5\text{-}13)$$

An exact solution of this equation, from a time of 0 to a time of t, yields

$$X_i = X_o - \tau_p (U_i - V_o + g_i \tau_p)[1 - \exp (- t / \tau_p)] + (U_i + g_i \tau_p) t \qquad (5\text{-}14)$$

$$V_i = - (U_i - V_o + g_i \tau_p) \exp (- t / \tau_p) + (U_i + g_i \tau_p) \qquad (5\text{-}15)$$

where

X_o = initial particle position

V_o = initial particle velocity

Similar equations may be written and solved for the turbulent correlations. Any step result serves as initial conditions for the next step integration, etc., through the entire simulation. The assumption that the background conditions U_i, $< x_i u_i >$ and $< u_i v_i >$ are constant across a time step permits solution of Equations (5-1) to (5-5) unrestricted by the size of the released material. Computational solution times are reduced significantly, and any drop size may be tracked by the equations.

FLOW FIELD MODELING

The behavior of the released material is intimately connected to the local background mean velocity U_i and turbulence field q^2 through which the material is transported. The near wake module in FSCBG contains a number of simplifications for the flow field velocity and turbulence levels additionally imposed in the aircraft wake. These models are summarized below.

Fixed-Wing Rolled Up Tip Vortices

When an aircraft flies at a constant altitude, the aerodynamic lift generated by the lifting surfaces of the aircraft equals the aircraft weight. The majority of the lift is carried by the wings, and generates one or more pairs of swirling masses of air (called vortices) downstream of the aircraft. If the roll-up of this trailing vorticity can be approximated as occurring immediately downstream of the wing, then the mean velocity field that results may be simply characterized by the aircraft semispan s, circulation Γ and load distribution. For a rectangularly loaded wing

$$\Gamma = \frac{W_t}{2 s \rho_A U_\infty} \qquad (5\text{-}16)$$

where

W_t = aircraft weight

U_∞ = aircraft flight speed

Vortex Circulation Decay

The flow field generated by a simply loaded wing includes four vortices: the two from either wing tip, and image vortices below the surface. The local ambient velocity from the vortices is the vector sum of the four swirl velocity components, each written as

$$V_S = \frac{\Gamma}{2\pi r} \tag{5-17}$$

with its direction perpendicular to a line connecting each vortex centroid and the observation point (the distance r). The observation point might be a particle position or the location of another vortex (which also moves because of the other vortices present in the flow). An inviscid vortex of constant positive circulation strength Γ_o descends toward the surface while increasing the separation distance between its companion vortex.

In the atmosphere, turbulence acts to decay the vortex strength. A simple decay model, developed in Donaldson and Bilanin 1975, results in a vortex decay of the form

$$\Gamma = \Gamma_o \exp\left(- \frac{Bqt}{s} \right) \tag{5-18}$$

For vortices out of ground effect, a typical value for $B = 0.41$; while a detailed examination of Program WIND data in ground effect (Bilanin et al. 1989) gives $Bq = 0.56$ m/sec.

Helicopter In Forward Flight

The helicopter model includes both hover downwash and the tip vortex pair by partitioning the helicopter weight between the two effects as a function of time. The hover downwash model is taken from actuator disk theory for a propeller and may be written as

$$F\, W_t = 2\, \pi\, \rho_A\, R^2\, w_d^2 \tag{5-19}$$

while the strength of the vortex pair may be found from

$$(1 - F)\, W_t = 2\, \rho_A\, R\, U_\infty\, \Gamma \tag{5-20}$$

where

W_t = helicopter weight

w_d = downwash at the rotor plane

R = radius of the rotor

Γ = tip circulation strength

The function F is determined from the expression

$$F = \exp\left(- \frac{k \mu \Gamma_o t}{\sigma \pi R^2} \right) \tag{5-21}$$

where

μ = forward advance ratio

σ = solidity

Γ_o = solution to Equation (5-20) for $F = 0$

The constant k relates helicopter roll-up (around a circumference at the blade tip) to fixed-wing roll-up. Predicted results from a helicopter wake model (Bliss, Teske and Quackenbush 1987) suggest that the downwash flow field quickly transitions (within two blade diameters) into a vortex pair. A typical value for $k = 7$.

The tip vortices influence the flow field everywhere, while the downwash affects only the spreading region beneath the rotor and the fluid column directly above the rotor. Within the boundaries of the rotor blade and the dividing streamline, the velocity is assumed to follow a stagnation point flow, while the vortex pair created by the helicopter is assumed to follow the dividing streamline.

Material released ahead of the helicopter (spray boom forward) is assumed to encounter a streamline pattern similar to flow around a circular cylinder (the actuator disk downwash, Kuethe and Schetzer 1964)

$$U = U_\infty \left(1 - \frac{R^2}{r^2} + \frac{2 R^2 y^2}{r^4} \right) \tag{5-22}$$

$$V = - \frac{2 U_\infty R^2 x y}{r^4} \tag{5-23}$$

until the material crosses the plane of the helicopter shaft centerline.

Jet Engine

The jet engine exhaust is modeled as a turbulent circular jet using the similarity analysis reported in Schlicting 1968. The results give the axial and radial velocities as

$$u_{axial} = \frac{3}{8\pi} \frac{\sqrt{\frac{T}{\rho_A}}}{\varepsilon x} \frac{1}{\left(1 + \frac{\eta^2}{4}\right)^2} \tag{5-24}$$

$$v_{radial} = \frac{1}{4} \sqrt{\frac{3}{\pi}} \frac{\sqrt{\frac{T}{\rho_A}}}{x} \frac{\left(\eta - \frac{\eta^3}{4}\right)}{\left(1 + \frac{\eta^2}{4}\right)^2} \tag{5-25}$$

with

$$\eta = \frac{1}{4} \sqrt{\frac{3}{\pi}} \frac{\sqrt{\frac{T}{\rho_A}}}{\varepsilon} \frac{r}{x} \tag{5-26}$$

$$\varepsilon = 0.0161 \sqrt{\frac{T}{\rho_A}} \tag{5-27}$$

where T is the jet thrust and x is the downstream distance corrected for the virtual origin. The radial velocity v_{radial} becomes part of the local fluid velocity, while the axial velocity u_{axial} is also used to evaluate the turbulence level within the jet exhaust

$$q^2 = 0.2034\, u_{axial}^2 \tag{5-28}$$

where the proportionality constant is determined from the centerline decay of turbulence in a free jet (Wygnanski and Fiedler 1969).

Propeller

The propeller is modeled as an actuator disk, where the incremental velocity ΔU above the flight speed U_∞ is related to the actual thrust produced by the propeller

$$T = 2\,\pi\,\rho_A\,R^2\,\Delta U\left(U_\infty + \Delta U\right) \tag{5-29}$$

where R is the radius of the propeller. In steady flight the thrust equals the aircraft drag, so that

$$T = C_D\,\frac{1}{2}\,\rho_A\,U_\infty^2\,S \tag{5-30}$$

where S is the wing planform area and C_D is the aircraft drag coefficient. Combining Equations (5-29) and (5-30) to eliminate thrust, results in

$$\frac{\Delta U}{U_\infty} = \frac{1}{2}\left(-1 + \sqrt{1 + \frac{C_D\,S}{\pi\,R^2}}\right) \tag{5-31}$$

An alternate expression for ε, defined in Equation (5-27), may be obtained from Schlicting 1968 as

$$\varepsilon = 0.0256\,R\,\Delta U \tag{5-32}$$

Combining this equation with Equation (5-27) gives the effective thrust level for the propeller as

$$T_{eff} = 2.5275\,\rho_A\,R^2\,\Delta U^2 \tag{5-33}$$

to permit the use of Equations (5-24) to (5-28) for the propeller when Equation (5-33) is substituted for T. The swirl velocity generated by the propeller is assumed to be linear in R out to its maximum value, and then zero for larger values of r. The resulting integration for swirl energy yields

$$V_{tip} = \frac{U_\infty^3 C_D S}{\pi \eta \Omega R^3 \left(U_\infty + \Delta U \right)} \tag{5-34}$$

where η is the propeller efficiency and Ω is the propeller rotation rate.

DEPOSITION MODELING

As material approaches the surface, deposition begins, and continues until all material is deposited (if evaporation occurs, some of the material will be left in the atmosphere to drift). Ground deposition is computed by assuming that the concentration of material around the mean may be taken as gaussian

$$C = \frac{1}{2 \pi \sigma^2} \exp\left[- \frac{(y - Y)^2}{2 \sigma^2} \right] \exp\left[- \frac{(z - Z)^2}{2 \sigma^2} \right] \tag{5-35}$$

where the released material is at position (Y,Z), and the standard deviation is σ. Thus, as the material approaches the surface, it deposits incrementally, and continues depositing at its approach rate after impact. Equation (5-35) is integrated from far below the surface to the material location to give

$$M_{plane} = \frac{1}{2 \sqrt{2} \pi \sigma} \exp\left[- \frac{(y - Y)^2}{2 \sigma^2} \right] \text{erfc}\left(\frac{Z}{\sqrt{2} \sigma} \right) \tag{5-36}$$

where erfc is the complementary error function. Ground deposition is obtained by summing all incremental contributions to M_{plane} as the integration proceeds. It may be seen that for material falling vertically toward the surface, the ground deposition pattern generated by Equation (5-36) will be identical to a gaussian deposition pattern. The use of Equation (5-36) leads to more realistic ground deposition distributions when the particles are traveling with nonzero horizontal velocities.

6. Dispersion

The spray dispersion models incorporated into FSCBG are similar to aircraft spray models described by Dumbauld, Rafferty and Cramer 1976. These models were developed previously for the U. S. Army Dugway Proving Ground and are based on the generalized diffusion model concepts described by Cramer et al. 1972. These models were also used in the CBG computer program, with their mathematical basis given in Appendix B of the report by Dumbauld, Rafferty and Bjorklund 1977. These models calculate peak concentration, dosage and deposition downwind from nearly-instantaneous elevated line sources oriented at an arbitrary angle with respect to the mean wind direction. The axis of the spray cloud is assumed to be inclined from the horizontal plane by an angle that is proportional to $V_j / \bar{u}$, where V_j is the gravitational settling velocity for the jth drop size category and $\bar{u}$ is the mean transport wind speed (above the canopy). When evaporation is negligible, this inclination angle is invariant with distance from the line source. For evaporating drops the angle changes with distance from the source because V_j depends on the size of the drop. It is assumed that drops dispersed upwards by turbulence are totally reflected downwards at the top of the surface mixing layer, but the fraction of drops reflected at the ground is a variable input parameter for each drop size category. The models use a Cartesian coordinate system for a line source of length L at a release height H and a calculation point at $R(\varepsilon,\delta,z)$ as shown in Figure 6-1.

VOLUME SOURCE MODELS

With these assumptions, the dosage for an instantaneous volume source is given by the expression

$$DOS_V = \frac{Q_V}{2\,\pi\,\sigma_y\,\sigma_z\,\bar{u}} \exp\left[-\frac{1}{2}\left(\frac{y}{\sigma_y}\right)^2\right] \sum_{j=1}^{NJ} f_j\, A(x,z) \qquad (6\text{-}1)$$

where

$$A(x,z) = \sum_{i=0}^{\infty} \gamma_j^{\,i} \exp\left[-\frac{1}{2}\left(\frac{2\,i\,H_m - H + z + \frac{V_j\,x}{\bar{u}}}{\sigma_z}\right)^2\right]$$

$$+ \sum_{i=0}^{\infty} \gamma_j^{\,i+1} \exp\left[-\frac{1}{2}\left(\frac{2\,i\,H_m + H + z - \frac{V_j\,x}{\bar{u}}}{\sigma_z}\right)^2\right]$$

$$+ \sum_{i=1}^{\infty} \gamma_j^{\,i} \exp\left[-\frac{1}{2}\left(\frac{2\,i\,H_m + H - z - \frac{V_j\,x}{\bar{u}}}{\sigma_z}\right)^2\right]$$

$$+ \sum_{i=1}^{\infty} \gamma_j^{i-1} \exp\left[-\frac{1}{2}\left(\frac{2\,i\,H_m - H - z + \frac{V_j\,x}{\bar{u}}}{\sigma_z} \right)^2 \right] \qquad (6\text{-}2)$$

and

Q_V = strength of the volume source

σ_y = standard deviation of the crosswind spray distribution

σ_z = standard deviation of the vertical spray distribution

x,y,z = the alongwind, crosswind and vertical coordinates of the point at which the dosage is calculated

f_j = mass fraction of the total source strength in the jth dropsize category (total number of dropsizes is NJ)

γ_j = reflection coefficient for the median drop by mass in the jth dropsize category (Figure 6-2)

H_m = depth of the surface mixing layer beneath a capping inversion

The lateral and vertical growth of the spray cloud due to turbulent mixing is assumed to be rectilinear. The expressions for σ_y and σ_z then become

$$\sigma_y = \sigma_A (x + x_V) \qquad (6\text{-}3)$$

$$\sigma_z = \sigma_E (x + x_V) = \frac{\sigma_A (x + x_V)}{k} \qquad (6\text{-}4)$$

where

σ_A = standard deviation of the wind azimuth angle (in radians)

σ_E = standard deviation of the wind elevation angle (in radians)

$$k = \frac{\sigma_A}{\sigma_E} \qquad (6\text{-}5)$$

$$x_v = \text{virtual distance} = \frac{k\,\sigma_o}{\sigma_A} - x_R = \frac{\sigma_o}{\sigma_E} - x_R \qquad (6\text{-}6)$$

and

σ_o = standard deviation of the cloud distribution at the distance x_R

x_R = distance downwind from the volume point source

The amount of spray material deposited on the ground or entering the forest canopy through gravitational settling is obtained from the expression

$$DEP_V = \frac{Q_V}{\sqrt{2\pi}\,\sigma_y} \exp\left[-\frac{1}{2}\left(\frac{y}{\sigma_y}\right)^2\right] \sum_{j=1}^{NJ} f_j \frac{d}{dx}\left[\frac{1}{\sqrt{2\pi}\,\sigma_z} \int_{-\infty}^{0} A(x,z)\,dz \right] \qquad (6\text{-}7)$$

After substitutions for σ_y and σ_z into Equation (6-7), and performing the indicated integration and differentiation, the deposition equation takes the form

$$DEP_V = \frac{k\,Q_V}{2\pi\,\sigma_A^2\,(x+x_v)^3} \exp\left[-\frac{1}{2}\left(\frac{y}{\sigma_A\,(x+x_v)}\right)^2\right] \sum_{j=1}^{NJ} f_j\,(1-\gamma_j)\,[MM+NN] \qquad (6\text{-}8)$$

where

$$MM = \left[H + \frac{V_j\,x_v}{\bar{u}} \right] \exp\left[-\frac{k^2}{2}\left(\frac{H - \frac{V_j\,x}{\bar{u}}}{\sigma_A\,(x+x_v)} \right)^2 \right] \qquad (6\text{-}9)$$

$$NN = \sum_{i=1}^{\infty} \gamma_j^{i-1} \left[2\,i\,H_m - H - \frac{V_j\,x_v}{\bar{u}} \right] \exp\left[-\frac{k^2}{2}\left(\frac{2\,i\,H_m - H + \frac{V_j\,x}{\bar{u}}}{\sigma_A\,(x+x_v)} \right)^2 \right]$$

$$+ \sum_{i=1}^{\infty} \gamma_j^i \left[2\,i\,H_m + H + \frac{V_j\,x_v}{\bar{u}} \right] \exp\left[-\frac{k^2}{2} \left(\frac{2\,i\,H_m + H - \frac{V_j\,x}{\bar{u}}}{\sigma_A\,(x + x_v)} \right)^2 \right] \qquad (6\text{-}10)$$

LINE SOURCE MODELS

The expressions for dosage and deposition downwind from a line source oriented at an arbitrary angle θ with the wind direction are derived through consideration of the line source geometry shown in Figure 6-1. A finite line source of length L is directed along the δ coordinate at height H with one end of the line source at the point $\varepsilon = 0$, $\delta = 0$ and $z = H$. From the geometry shown in Figure 6-1, it may be seen that

$$x = x' - \delta' \sin\theta \qquad (6\text{-}11)$$

$$y = \delta' \cos\theta + x' \tan\theta - \frac{\delta}{\cos\theta} \qquad (6\text{-}12)$$

$$x' = \varepsilon \cos\theta + \delta \sin\theta \qquad (6\text{-}13)$$

When Equations (6-11), (6-12) and (6-13) are substituted for x, y and x' in Equations (6-1) and (6-8), the dosage and deposition at any point R downwind from the line source becomes

$$DOS_L = \int_0^L DOS_V \, d\delta' \qquad (6\text{-}14)$$

$$DEP_L = \int_0^L DEP_V \, d\delta' \qquad (6\text{-}15)$$

The solution procedure is laborious, but leads to the following expressions.

DOSAGE ABOVE CANOPY

The dosage (mass times time divided by volume) above the canopy is the sum of contributions from drops in the dispersing cloud and from vapor produced by drop

evaporation. The above canopy dosage for the contribution from drops is given by the expression

$$DOS_L = \frac{S}{k\,\sigma_A \sin\theta\,\bar{u}} \sum_{j=1}^{NJ} f_j \left\{ \sum_{i=0}^{\infty} \left[\gamma_j^i \left(\frac{\pi}{2Y}\right)^{1/2} \exp\left(\frac{O^2}{4Y} - P\right) \left\{ \operatorname{erf}\left(\sqrt{Y}\left(\frac{k}{b} + \frac{O}{2Y}\right)\right) - \operatorname{erf}\left(\sqrt{Y}\left(\frac{k}{a} + \frac{O}{2Y}\right)\right)\right\} \right.\right.$$
$$+ \gamma_j^{i+1} \left(\frac{\pi}{2Z}\right)^{1/2} \exp\left(\frac{R^2}{4Z} - P\right) \left\{ \operatorname{erf}\left(\sqrt{Z}\left(\frac{k}{b} + \frac{R}{2Z}\right)\right) - \operatorname{erf}\left(\sqrt{Z}\left(\frac{k}{a} + \frac{R}{2Z}\right)\right)\right\} \Big]$$
$$+ \sum_{i=1}^{\infty} \left[\gamma_j^i \left(\frac{\pi}{2T}\right)^{1/2} \exp\left(\frac{U^2}{4T} - P\right) \left\{ \operatorname{erf}\left(\sqrt{T}\left(\frac{k}{b} + \frac{U}{2T}\right)\right) - \operatorname{erf}\left(\sqrt{T}\left(\frac{k}{a} + \frac{U}{2T}\right)\right)\right\} \right.$$
$$\left. + \gamma_j^{i-1} \left(\frac{\pi}{2W}\right)^{1/2} \exp\left(\frac{X^2}{4W} - P\right) \left\{ \operatorname{erf}\left(\sqrt{W}\left(\frac{k}{b} + \frac{X}{2W}\right)\right) - \operatorname{erf}\left(\sqrt{W}\left(\frac{k}{a} + \frac{X}{2W}\right)\right)\right\} \right] \Big] \Big\} \tag{6-16}$$

where

$$a = \sqrt{2}\,\sigma_A (x' + x_v) \tag{6-17}$$

$$b = \sqrt{2}\,\sigma_A (x' + x_v - \ell \sin\theta) \tag{6-18}$$

$$C = 2\,i\,H_m - H - \frac{V_j\,x_v}{\bar{u}} \tag{6-19}$$

$$D = 2\,i\,H_m + H + \frac{V_j\,x_v}{\bar{u}} \tag{6-20}$$

$$N = (x' + x_v)\cot\theta + x' \tan\theta - \frac{\delta}{\cos\theta} \tag{6-21}$$

$$S = \frac{Q_V k}{2\pi} \tag{6-22}$$

$$O = \frac{\sqrt{2}}{\sigma_A k}\left[\frac{k^2 V_j}{\bar{u}}(C+z) - N\cot\theta\right] \tag{6-23}$$

$$P = \frac{1}{2\sigma_A^2}\left\{\left[\frac{k V_j}{\bar{u}}\right]^2 + [\cot\theta]^2\right\} \tag{6-24}$$

$$R = -\frac{\sqrt{2}}{\sigma_A k}\left[\frac{k^2 V_j}{\bar{u}}(D+z) + N\cot\theta\right] \tag{6-25}$$

$$T = \frac{N^2}{k^2} + [D-z]^2 \tag{6-26}$$

$$U = -\frac{\sqrt{2}}{\sigma_A k}\left[\frac{k^2 V_j}{\bar{u}}(D-z) + N\cot\theta\right] \tag{6-27}$$

$$W = \frac{N^2}{k^2} + [C-z]^2 \tag{6-28}$$

$$X = \frac{\sqrt{2}}{\sigma_A k}\left[\frac{k^2 V_j}{\bar{u}}(C-z) - N\cot\theta\right] \tag{6-29}$$

$$Y = \frac{N^2}{k^2} + [C+z]^2 \tag{6-30}$$

$$Z = \frac{N^2}{k^2} + [D+z]^2 \tag{6-31}$$

ℓ = effective line length

$$= \begin{cases} \delta + \varepsilon\cot\theta \; ; \; \delta + \varepsilon\cot\theta \le L \\ L \qquad\qquad ; \; \delta + \varepsilon\cot\theta > L \end{cases} \tag{6-32}$$

As inspection of Equation (6-16) and the definitions of the parameters appearing in the equation show that the model cannot be used when the wind direction is exactly parallel to the line source ($\theta = 90$ degrees) or when the wind direction is exactly perpendicular to the line source ($\theta = 0$ degrees). For the case when $\theta = 90$ degrees, FSCBG uses the exact solution by making the following observations (from Figure 6-1 with rotation of the wind to along the line source)

$$x = x' - \delta$$

$$y = \varepsilon$$

$$x' = \delta$$

$$\cos\theta = 0 \qquad (6\text{-}33)$$

$$N = \varepsilon$$

$$\sin\theta = 1$$

and defining x' as the downwind distance from the upwind edge of the line source and y as the crosswind distance from the line source (perpendicular). Equation (6-16) then applies with these substitutions.

For the case $\theta = 0$ degrees, FSCBG also uses the exact solution, with

$$x = \varepsilon$$

$$y = \delta' - \delta \qquad (6\text{-}34)$$

$$x' = \varepsilon$$

where x is now the downwind (perpendicular) distance from the line source and y is the crosswind distance from the center of the line source. In this limit the standard deviations of the crosswind distribution σ_y and vertical distribution σ_z are defined by the expressions

$$\sigma_y = \sigma_A x + \sigma_o \qquad (6\text{-}35)$$

$$\sigma_z = \sigma_E x + \sigma_o \qquad (6\text{-}36)$$

The result becomes

$$DOS_L = \frac{Q_V}{\sqrt{2\pi}\,\sigma_z\,\bar{u}} \sum_{j=1}^{NJ} f_i \frac{1}{2}\left[\operatorname{erf}\left(\frac{L/2 + y}{\sqrt{2}\,\sigma_y} \right) + \operatorname{erf}\left(\frac{L/2 - y}{\sqrt{2}\,\sigma_y} \right) \right] A(x,z) \qquad (6\text{-}37)$$

Vapor emitted from evaporating drops also contributes to the total dosage above the canopy. In FSCBG the evaporation model determines the mass of vapor emitted in Δh height units along the cloud axis as it descends to the canopy. The distance downwind from the line source where the vapor is emitted is given by $\bar{u}\,t$ where t is the time from the evaporation model when the cloud axis passes through the midpoint of the height interval Δh. The source dimension of the vapor cloud emitted over the Δh height interval is defined by

$$\sigma_o = \frac{\Delta h}{\sqrt{12}} \qquad (6\text{-}38)$$

under the assumption that the vapor is rectangularly distributed at the point of emission. The vapor dosage contribution is then calculated from the appropriate equations with $V_j = 0$, $\gamma_j = 1$, and $x_R = \bar{u}\,t$. The total dosage at each calculation point is determined by summing the contributions from drops and vapor.

DEPOSITION ABOVE AND WITHIN CANOPY

The deposition (mass divided by area) above the canopy is given by the expression

$$DEP_L = \frac{2S}{\sin\theta} \sum_{j=1}^{NJ} f_j (1 - \gamma_j) \left\{ \frac{B \exp\left(\frac{G^2}{4F} - P \right)}{2F} \right.$$

$$\left[\exp\left(-F\left(\frac{1}{a} - \frac{G}{2F} \right)^2 \right) - \exp\left(-F\left(\frac{1}{b} - \frac{G}{2F} \right)^2 \right) \right.$$

$$\left. \left. + \frac{G\sqrt{\pi}}{2\sqrt{F}} \left[\operatorname{erf}\left(\sqrt{F}\left(\frac{1}{b} - \frac{G}{2F} \right) \right) - \operatorname{erf}\left(\sqrt{F}\left(\frac{1}{a} - \frac{G}{2F} \right) \right) \right] \right]$$

$$+ \sum_{i=1}^{\infty} \gamma_j^{i-1} \frac{C \exp\left(\frac{J^2}{4I} - P \right)}{2I}$$

$$\left[\exp\left(-I\left(\frac{1}{a} - \frac{J}{2I} \right)^2 \right) - \exp\left(-I\left(\frac{1}{b} - \frac{J}{2I} \right)^2 \right) \right.$$

$$+\frac{I\sqrt{\pi}}{2\sqrt{I}}\left[\operatorname{erf}\left(\sqrt{I}\left(\frac{1}{b}-\frac{J}{2I}\right)\right)-\operatorname{erf}\left(\sqrt{I}\left(\frac{1}{a}-\frac{J}{2I}\right)\right)\right]\Bigg]$$

$$+\sum_{i=1}^{\infty}\gamma_j^i\frac{D\exp\left(\frac{K^2}{4E}-P\right)}{2E}$$

$$\left[\exp\left(-E\left(\frac{1}{a}-\frac{K}{2E}\right)^2\right)-\exp\left(-E\left(\frac{1}{b}-\frac{K}{2E}\right)^2\right)\right.$$

$$\left.+\frac{K\sqrt{\pi}}{2\sqrt{E}}\left[\operatorname{erf}\left(\sqrt{E}\left(\frac{1}{b}-\frac{K}{2E}\right)\right)-\operatorname{erf}\left(\sqrt{E}\left(\frac{1}{a}-\frac{K}{2E}\right)\right)\right]\right]\Bigg\} \qquad (6\text{-}39)$$

with the same substitutions as before, in addition to

$$B = H + \frac{V_j x_v}{\bar{u}} \qquad (6\text{-}40)$$

$$E = k^2 D^2 + N^2 \qquad (6\text{-}41)$$

$$F = k^2 B^2 + N^2 \qquad (6\text{-}42)$$

$$G = \frac{\sqrt{2}}{\sigma_A}\left[\frac{V_j B k^2}{\bar{u}} + N\cot\theta\right] \qquad (6\text{-}43)$$

$$I = k^2 C^2 + N^2 \qquad (6\text{-}44)$$

$$J = -\frac{\sqrt{2}}{\sigma_A}\left[\frac{V_j C k^2}{\bar{u}} + N\cot\theta\right] \qquad (6\text{-}45)$$

$$K = \frac{\sqrt{2}}{\sigma_A}\left[\frac{V_j D k^2}{\bar{u}} + N\cot\theta\right] \qquad (6\text{-}46)$$

The deposition model that applies when the wind direction is exactly parallel to the line source may be obtained from Equation (6-39) using the substitutions defined by Equation (6-33). Deposition for the case when the wind is exactly perpendicular to the line source is found using the substitutions defined by Equation (6-34), resulting in

$$DEP_L = \frac{Q_V}{\sqrt{2\pi}\,\sigma_z} \sum_{j=1}^{NJ} f_i\,(1-\gamma_j)\,\frac{1}{2}\left[\mathrm{erf}\left(\frac{L/2+y}{\sqrt{2}\,\sigma_y}\right)+\mathrm{erf}\left(\frac{L/2-y}{\sqrt{2}\,\sigma_y}\right)\right]$$

$$\left\{\left[H+\frac{V_j x_v}{\bar{u}}\right]\exp\left(-\frac{1}{2}\left(\frac{H-\frac{V_j x}{\bar{u}}}{\sigma_z}\right)^2\right)\right.$$

$$+\sum_{i=1}^{\infty}\gamma_j^{i-1}\left[2\,i\,H_m-H-\frac{V_j x_v}{\bar{u}}\right]\exp\left(-\frac{1}{2}\left(\frac{2\,i\,H_m-H+\frac{V_j x}{\bar{u}}}{\sigma_z}\right)^2\right)$$

$$\left.+\sum_{i=1}^{\infty}\gamma_j^{i}\left[2\,i\,H_m+H+\frac{V_j x_v}{\bar{u}}\right]\exp\left(-\frac{1}{2}\left(\frac{2\,i\,H_m+H-\frac{V_j x}{\bar{u}}}{\sigma_z}\right)^2\right)\right\} \qquad (6\text{-}47)$$

Again, x is the downwind distance from the source and y is the crosswind distance from the center of the line source; σ_y and σ_z are defined by Equations (6-35) and (6-36).

DOSAGE WITHIN CANOPY

In calculating within-canopy deposition, FSCBG makes the simplifying assumption that the effects of within-canopy diffusion are negligible. Thus, drops that penetrate through the canopy are assumed to follow simple ballistic trajectories. Deposition within the canopy is related to deposition above the canopy by a canopy penetration algorithm that determines the fraction of drops in each size category that reach a given height within the canopy (Section 4).

To compute dosage within a canopy, Bowers 1991 suggests that with simplifying assumptions

$$DOS_L = \frac{DEP_L}{V_j} \qquad (6\text{-}48)$$

EVAPORATION EFFECTS WITHIN CANOPY

When no evaporation occurs, the calculation of deposition using Equation (6-39) is relatively straightforward because the gravitational settling velocity V_j is invariant with time. However, when evaporation occurs, both dropsize and gravitational velocity vary with travel distance from the source, and the deposition calculations become more complicated. Within a canopy FSCBG follows a stepwise procedure for each jth dropsize as summarized below.

1. FSCBG uses the above-canopy (open terrain) evaporation model described in Section 3 to establish a quadratic curve relating the gravitational settling velocity V_j of the median drop in the jth dropsize category as a function of travel distance x from the source for above-canopy meteorology.

2. The above-canopy evaporation model is also used to calculate the height trajectory of the jth dropsize as a quadratic function of travel distance.

3. The within-canopy evaporation model is used to calculate the trajectory of the median drop in the jth dropsize category, using within-canopy meteorology and assuming that the drop entered the canopy with the settling velocity V_{jc} given by the above-canopy evaporation model at the canopy height. In addition to calculating the mass loss within the canopy, the within-canopy evaporation model calculates the travel distance of the median drop from the time it enters the canopy until it strikes the ground.

4. FSCBG internally develops a curve relating the difference between the receptor distance from the source and the travel distance in the canopy for all dropsize categories versus the settling velocity at the canopy top V_{jc} for each jth category.

5. The intersection of the curve developed in Step 4 and the above-canopy evaporation curve for the jth dropsize category defines the distance x_{eff} from the source to the point where the jth median drop would have to enter the canopy in order to reach the calculation point.

6. The effective height H_{eff} of the cloud centroid for the jth dropsize category at the distance from the source determined in Step 5 is obtained from the height versus distance curve determined in Step 2.

7. The deposition model equations yield the corrected deposition values when an effective value of V_j is used. This effective value is found from the expression

$$V_j = \frac{\bar{u}\,(H - H_{eff})}{x_{eff}} \qquad (6\text{-}49)$$

The calculations then proceed in the usual fashion except for appropriate adjustments for mass loss due to canopy impaction.

PEAK CONCENTRATION

The peak concentration (mass divided by volume) which occurs at the calculation point is determined from the expression

$$CON_{LP} = \frac{DOS_L\,\bar{u}}{\sqrt{2}\,\sigma_x} \qquad (6\text{-}50)$$

where σ_x is the standard deviation of the cloud in the alongwind direction defined by

$$\sigma_x = \left[\left(\frac{L(x)}{4.3} \right)^2 + \sigma_\delta^2 \right]^{1/2} \tag{6-51}$$

and

$L(x)$ = alongwind cloud length

$$= \frac{0.6\,\Delta\bar{u}}{\bar{u}} \left(x' - \frac{L \sin\theta}{2} \right) \tag{6-52}$$

$\Delta\bar{u}$ = vertical wind-speed shear in the layer containing the cloud

Peak concentrations obtained using FSCBG are strictly correct only for crosswind releases. Errors made for alongwind releases and releases at an angle to the wind direction decrease at distances beyond the more downwind end of the line source.

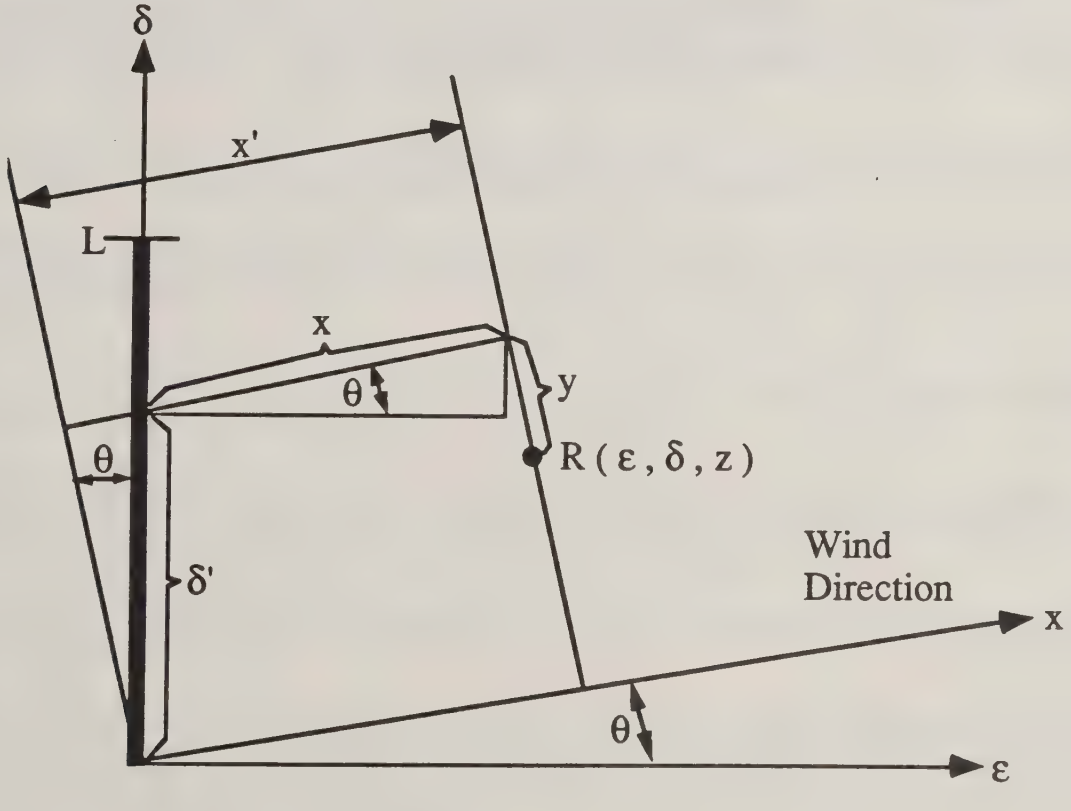

Figure 6-1. Line source geometry.

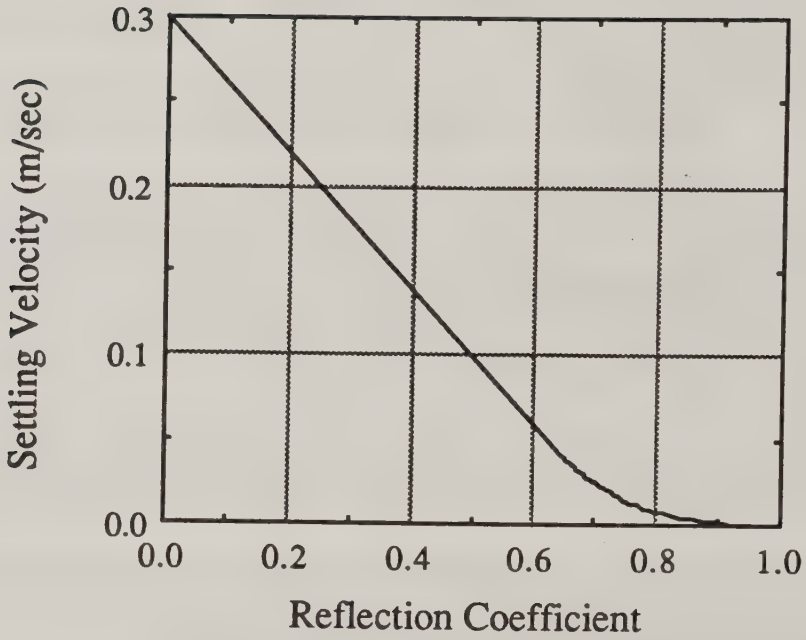

Figure 6-2. Relationship between the gravitational settling velocity Vj and the reflection coefficient γ_i at the ground (from Dumbauld, Rafferty and Cramer 1976).

7. References

Barnhill, R. E. 1977: "Representation and Approximation of Surfaces," Mathematical Software III (J. R. Rice ed.), Academic Press, New York, pp. 69-120.

Beard, K. V. and H. R. Pruppacher 1971: "A Wind Tunnel Investigation of the Rate of Evaporation of Small Water Drops Falling at Terminal Velocity in Air," Journal of the Atmospheric Sciences, Vol. 28, pp. 1455-1464.

Bergen, J. D. 1971: "Vertical Profiles of Windspeed in a Pine Stand," Forest Science, 17, pp. 314-321.

Bilanin, A. J. and M. E. Teske 1984: "Numerical Studies of the Deposition of Material Released from Fixed and Rotary Wing Aircraft," NASA CR 3779.

Bilanin, A. J., M. E. Teske, J. W. Barry and R. B. Ekblad 1989: "Project WIND Anemometer Tower Flyby Data Reduction," American Meteorological Society Conference on Agricultural and Forest Meteorology, Charleston, pp. 188-191.

Bjorklund, J. R., C. R. Bowman and G. C. Dodd 1988: "User Manual for the FSCBG Aircraft Spray and Dispersion Model Version 2.0," USDA Forest Service Forest Pest Management Report No. FPM-88-5.

Bjorklund, J. R., C. R. Bowman and R. K. Dumbauld 1984: "User's Manual for the Mesoscale Wind Field Model Statistical Evaluation Computer Program (MWMSE)," H. E. Cramer Company, Inc. Technical Report No. TR-84-347-01.

Bliss, D. B., M. E. Teske and T. R. Quackenbush 1987: "A New Methodology for Free Wake Analysis Using Curved Vortex Elements," NASA CR 3958.

Bowers, J. F. 1991: "On the Estimation of Below-Canopy Drop Dosages from FSCBG Model Deposition Predictions," U. S. Army Dugway Proving Ground Technical Note No. 91-90-2.

Cionco, R. M. 1965: "A Mathematical Model for Air Flow in a Vegetative Canopy," Journal of Applied Meteorology, Vol. 4, pp. 517-522.

Cramer, H. E., J. R. Bjorklund, F. A. Record, R. K. Dumbauld, R. N. Swanson, J. E. Faulkner and A. G. Tingle 1972: "Development of Dosage Models and Concepts," U. S. Army Dugway Proving Ground Report No. DTC-TR-72-609-I and II.

Donaldson, C. duP. and A. J. Bilanin 1975: "Vortex Wakes of Conventional Aircraft," AGARDograph No. 204.

Dumbauld, R. K., J. R. Bjorklund and S. F. Saterlie 1980: "Computer Models for Predicting Aircraft Spray Dispersion and Deposition Above and Within Forest Canopies: Users Manual for the FSCBG Computer Program," USDA Forest Service Methods Application Group Report No. 80-11.

Dumbauld, R. K. and J. F. Bowers 1983: "Functional Methodologies for Characterizing Wind-Speed, Turbulence Profiles and Turbulent Diffusion Coefficients Within and Above

Vegetation Canopies and Urban Domains," H. E. Cramer Company, Inc. Technical Report No. TR-83-341-01.

Dumbauld, R. K., J. E. Rafferty and J. R. Bjorklund 1977: "Prediction of Spray Behavior Above and Within a Forest Canopy," H. E. Cramer Company, Inc. Report No. TR-77-308-01.

Dumbauld, R. K., J. E. Rafferty and H. E. Cramer 1976: "Dispersion - Deposition from Aerial Spray Releases," American Meteorological Society Third Symposium on Atmospheric Turbulence, Diffusion and Air Quality, Raleigh, pp. 520-527.

Fuchs, N. A. 1959: Evaporation and Droplet Growth in Gaseous Media, Pergamon Press, New York, 72 pp.

Goering, C. E., L. E. Bode and M. R. Gebhardt 1972: "Mathematical Modeling of Spray Droplet Deceleration and Evaporation," Transactions of the ASAE, pp. 220-225.

Golovin, M. N. and A. A. Putnam 1962: "Inertial Impaction on Single Elements," I&EC Fundamentals, Vol. 1, No. 4, pp. 264-273.

Gregory, J. A. 1974: "Smooth Interpolation Without Twist Constraints," Computer Aided Geometric Design (R. E. Barnhill and R. F. Riesenfeld eds.), Academic Press, New York, pp. 71-87.

Hall, W. D. and H. R. Pruppacher 1976: "The Survival of Ice Particles Falling from Cirrus Clouds in Subsaturated Air," Journal of the Atmospheric Sciences, Vol. 33, pp. 1995-2006.

Hardy, R. L. 1971: "Multiquadric Equations of Topography and Other Irregular Surfaces," Journal of Geophysical Research, Vol. 76, pp. 1905-1915.

Kuethe, A. M. and J. D. Schetzer 1964: Foundations of Aerodynamics, John Wiley and Sons, pp. 64-65.

Langmuir, I. and K. B. Blodgett 1946: "A Mathematical Investigation of Water Droplet Trajectories," AAF TR No. 5418 (Contract No. W-33-038-ac-9151), Air Technical Service Command, Army Air Force.

McDonald, J. E. 1960: "An Aid to Computation of Terminal Fall Velocities of Spheres," Journal of Meteorology, Vol. 17, pp. 463-465.

Pruppacher, H. R. and R. Rasmussen 1979: "A Wind Tunnel Investigation of the Rate of Evaporation of Large Water Drops Falling at Terminal Velocity in Air," Journal of the Atmospheric Sciences, Vol. 36, pp. 1255-1260.

Pulley, R. A. and J. K. Walters 1990: "The Effect of Interception on Pesticide Collection by Spheres and Cylinders," Journal of Aerosol Science, Vol. 21, No. 6, pp. 733-743.

Rafferty, J. E. and J. F. Bowers 1989: "Comparison of FSCBG2 and FSCBG3 Aerial Spray Model Predictions with Field Measurements," U. S. Army Dugway Proving Ground Report No. DPG-FR-90-001.

Rasmussen, L. A. 1978: "On the Approximation of Saturation Vapor Pressure," Journal of Applied Meteorology, Vol. 19, pp. 1564-1565.

Schlicting, H. 1968: Boundary Layer Theory, McGraw-Hill, p. 747.

Teske, M. E. 1988: "AGDISP Mod 5.0 Solution Algorithm," Continuum Dynamics, Inc. Technical Note No. 88-10.

Teske, M. E. 1990: "AGDISP User Manual Mod 6.0," Continuum Dynamics, Inc. Technical Note No. 90-16.

von Karman, T. D. and L. Howarth 1938: "On the Statistical Theory of Isotropic Turbulence," Proceedings of the Royal Society of London (A), pp. 164.

Weast, R. C. (ed.) 1981: Handbook of Chemistry and Physics (62nd Edition), CRC Press Inc., Boca Raton, pp. D190-D193.

Williamson, R. B. and E. D. Threadgill 1974: "A Simulation for the Dynamics of Evaporating Spray Droplets in Agricultural Spraying," Transactions of the ASAE, pp. 254-261.

Wygnanski, I. and Fiedler, H. 1969: "Some Measurements in the Self-Preserving Jet," Journal of Fluid Mechanics, Vol. 38, pp. 577-612.